



Received 14 July 2023

Accepted 19 September 2023

Edited by C. Schulzke, Universität Greifswald,
Germany**Keywords:** crystal structure; Hirshfeld surface analysis; metallacycle; chelating *N,S*-ligands; Hg²⁺ complex.**CCDC reference:** 2296007**Supporting information:** this article has supporting information at journals.iucr.org/e

Crystal structure and Hirshfeld surface analysis of cyclo-tetrabromido-1κ²Br,3κ²Br-tetrakis(μ₂-2-[(pyridin-2-yl)methyl]amino)ethane-1-thiolato-κ³N,S:S)tetramercury(II)

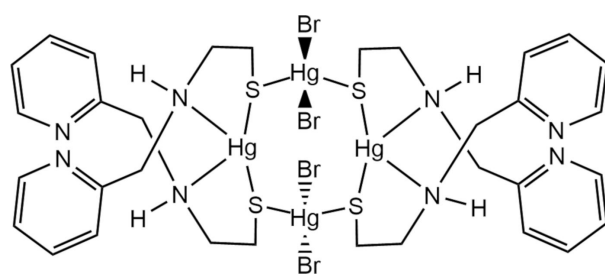
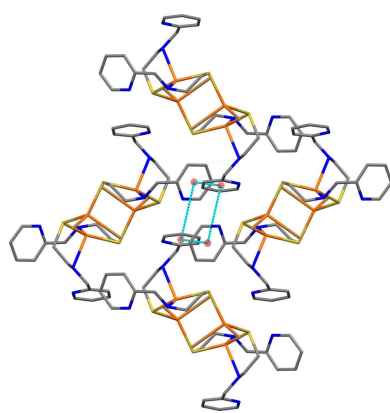
Isla D. Thomas, Kathryn R. Kocher, Julie A. Viehweg, Robert D. Pike and Deborah C. Bebout*

Department of Chemistry, William & Mary, Williamsburg, VA 23187-8795, USA. *Correspondence e-mail: dcbebo@wm.edu

The macrometallacyclic title compound, [Hg₄Br₄(C₈H₁₁N₂S)₄] or [(HgL₂)(HgBr₂)₂] (**1**) where **HL** = 2-[(pyridin-2-yl)methyl]amino)ethane-1-thiol, was prepared and structurally characterized. The Hg²⁺ complex crystallizes in the *P2*₁/*c* space group. The centrosymmetric Hg₄S₄ metallacycle is constructed from metal ions with alternating distorted tetrahedral Br₂S₂ and distorted seesaw N₂S₂ primary coordination environments with pendant pyridyl groups. The backfolded extended chair metallacycle conformation suggests interactions between each of the bis-chelated mercury atoms and Br atoms lying above and below the central Hg₂S₄ plane. Supramolecular interactions in **1** include a fourfold aryl embrace and potential hydrogen bonds with bromine as the acceptor. Hirshfeld surface analysis indicates that H···H (51.7%), Br···H/H···Br (23.0%) and C···H/H···C (9.5%) interactions are dominant.

1. Chemical context

For many years, we and others have been interested in the structures of group 12 coordination compounds including an aminoethanethiolate moiety (Hu *et al.*, 2020; Hallinger *et al.*, 2017; Akhtar *et al.*, 2015; Bharara *et al.*, 2006*a,b*; Fleischer *et al.*, 2006; Viehweg *et al.*, 2010; Brand & Vahrenkamp, 1995; Avdeef *et al.*, 1992; Tuntulani *et al.*, 1992; Kaptein *et al.*, 1987). Single-crystal X-ray diffraction is critical to the characterization of group 12 aminoethanethiolate complexes since the nuclearity of complexes with 1:1 metal-to-ligand ratio can vary with the identity of ancillary ligands and counter-ions (Brennan *et al.*, 2022; Lai *et al.*, 2013; Brand & Vahrenkamp, 1995) and complexes with novel ring structures have been produced (Ritz *et al.*, 2019; Viehweg *et al.*, 2010).



In contrast to the polymeric [ZnLX]_n structure reported for zinc halide complexes of deprotonated **HL** = 2-[(pyridin-2-yl)methyl]amino)ethane-1-thiol (Brand & Vahrenkamp, 1995), the cyclic tetrานuclear compound cyclo-tetrabromido-1κ²Br,3κ²Br-tetrakis(μ₂-2-[(pyridin-2-yl)methyl]amino)-



OPEN ACCESS

Published under a CC BY 4.0 licence

ethane-1-thiolato- $\kappa^3N,S:S$)tetramercury(II) (**1**) constructed from alternating Hg_2L_2 and $HgBr_2$ centers was found for the mercuric bromide complex of **L**. This communication reports the preparation, crystal structure, and Hirshfeld surface analysis of **1**, which facilitate an in-depth discussion of its structural features.

2. Structural commentary

Complex **1** crystallizes as discrete centrosymmetric molecules with an eight-membered metallacycle of alternating mercury and sulfur atoms (Fig. 1). The asymmetric unit contains $Hg_2L_2Br_2$, which is one half of complex **1**. The sets of four mercury(II) centers and four sulfur atoms in **1** each lie rigorously in their own plane, as required by the crystallographic inversion center located in the center of the molecule. The angle between these planes is $25.741 (18)^\circ$. The two Hg_2 atoms are approximately tetrahedrally coordinated to two terminal

Table 1
Selected geometric parameters (\AA , $^\circ$) for **1**.

$Hg\text{-}N2$	2.372 (3)	$Hg_2\text{-}S1$	2.4802 (9)
$Hg1\text{-}N4$	2.500 (3)	$Hg_2\text{-}S2^i$	2.4826 (9)
$Hg1\text{-}S1$	2.4646 (9)	$Hg_2\text{-}Br1$	2.6323 (4)
$Hg1\text{-}S2$	2.4348 (9)	$Hg_2\text{-}Br2$	2.7158 (4)
$N2\text{-}Hg1\text{-}N4$	112.59 (10)	$S1\text{-}Hg2\text{-}S2^i$	127.94 (3)
$N2\text{-}Hg1\text{-}S2$	115.39 (8)	$S1\text{-}Hg2\text{-}Br1$	108.19 (2)
$N4\text{-}Hg1\text{-}S1$	104.57 (7)	$S1\text{-}Hg2\text{-}Br2$	101.76 (2)
$N4\text{-}Hg1\text{-}S2$	82.25 (7)	$Br1\text{-}Hg2\text{-}S2^i$	105.56 (2)
$S1\text{-}Hg1\text{-}S2$	156.40 (3)	$Br2\text{-}Hg2\text{-}S2^i$	104.21 (2)
$Hg1\text{-}S1\text{-}Hg2$	96.99 (3)	$Br1\text{-}Hg2\text{-}Br2$	107.804 (12)
$Hg1\text{-}S2\text{-}Hg2^i$	97.38 (3)		

Symmetry code: (i) $-x + 1, -y + 1, -z + 1$

bromines and two bridging sulfur atoms (Table 1). These are separated by bis-chelated $Hg1$ metal atoms. The potentially tridentate ligand has an $N\text{-}\mu_2\text{-}S$ coordination mode with a pendant pyridyl ring. The pyridyl nitrogen atoms are located $3.563 (4)\text{--}4.303 (3)$ \AA from the closest mercury atoms and oriented unfavorably for either intra- or intermolecular bonding interactions with a metal center. The chelate rings have an envelope conformation with the methylene carbon in the flap position. The $Hg1$ metal atoms show a marked distortion from tetrahedral towards seesaw coordination with a widened $S\text{-}Hg\text{-}S$ angle of $156.40 (3)^\circ$. The two bridging $Hg\text{-}S$ distances are slightly longer and more similar ($\Delta = 0.003 \text{\AA}$) than the two chelating $Hg\text{-}S$ distances ($\Delta = 0.030 \text{\AA}$).

Alternatively, the Hg_4S_4 ring can be viewed as an extended chair containing a central planar Hg_2S_4 arrangement with one backfolded mercury atom on each side of the plane. The six Hg_2S_4 atoms lie between $0.0653 (3)$ and $0.1079 (5)$ \AA from the mean plane. The HgS_2 planes forming the head and foot of the chair are in an unusually acute $83.99 (4)^\circ$ angle with the central plane placing Hg_2 and Br_2 over the $Hg_1_2S_4$ plane. Furthermore, the $Hg_2\text{-}Br_2$ bonds are 0.084\AA longer than the $Hg_2\text{-}Br_1$ bonds. These observations imply some weak interactions between the Br_2 atoms and the two bis-chelated mercury atoms located $3.3951 (5)$ \AA and $3.6026 (5)$ \AA away. In a similar setting, such likely interactions between group 12 metal ions and halides have been reported for complexes of 2-(dimethylamino)ethanethiolate (Casals *et al.*, 1991). Furthermore, a related pentacyclic $Cd_4S_4Cl_2$ primary bonding core has been reported for $[(Cd(SC(CH_3)_2CH_2NH_2)_2(CdCl_2)]_2\cdot 2H_2O$ (refcode MEASCD; Fawcett *et al.*, 1978). The $Hg\cdots Hg$ separation between the bis-brominated mercury atoms [$5.0530 (6) \text{\AA}$] is shorter than the distance between the bis-chelated mercury atoms [$5.4023 (5) \text{\AA}$], both of which are too long for significant interactions between the metal atoms. In contrast, $[CuL]_4$ has mono- N,S chelated metal atoms in a D_{2d} butterfly arrangement with $Cu\cdots Cu$ separations of $2.6957 (11)$ and $3.370 (1) \text{\AA}$ (refcode TEVMAI; Stange *et al.*, 1996).

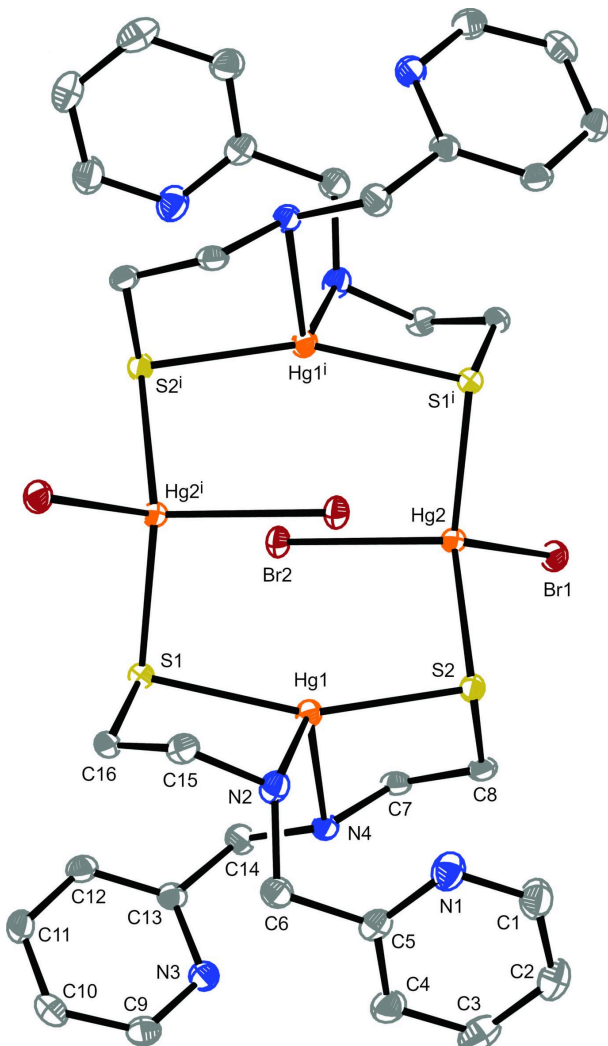


Figure 1

The molecular structure of **1** with the atom numbering scheme generated with ORTEP-3 for Windows (Farrugia, 2012). Displacement ellipsoids are drawn at the 50% probability level. Symmetry code: (i) $-x + 1, -y + 1, -z + 1$.

3. Supramolecular features

In addition to a variety of van der Waals contacts, the packing of **1** is stabilized by $\pi\cdots\pi$ interactions (Fig. 2 and Table 2) and

Table 2

Overview of pyridyl-pyridyl ring geometry metrics (\AA , $^\circ$) for **1**.

Cg1 and *Cg2* are the centroids of the N1/C1–C5 and N3/C9–C13 rings, respectively.

Centroids	Dihedral angle between rings	Centroid–centroid distance	Centroid–plane distance	Centroid offset
<i>Cg1</i> ··· <i>Cg2</i> ⁱ	62.87 (13)	4.873 (2)	4.735 (3)	1.151
<i>Cg1</i> ··· <i>Cg2</i> ⁱⁱ	62.87 (13)	4.453 (2)	4.312 (3)	1.112

Symmetry codes: (i) $x, y - \frac{1}{2}, -z + \frac{1}{2}$; (ii) $x, -y + \frac{3}{2}, z + \frac{1}{2}$.

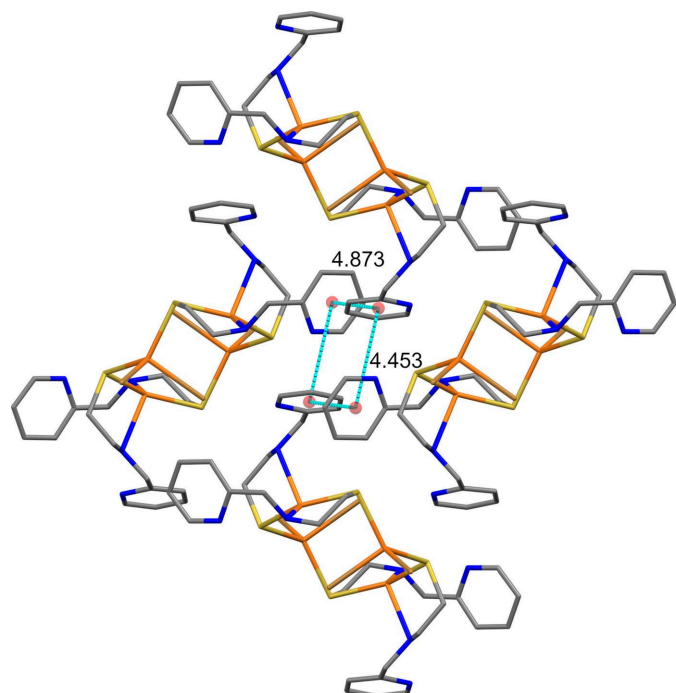
Table 3

Hydrogen-bond geometry (\AA , $^\circ$).

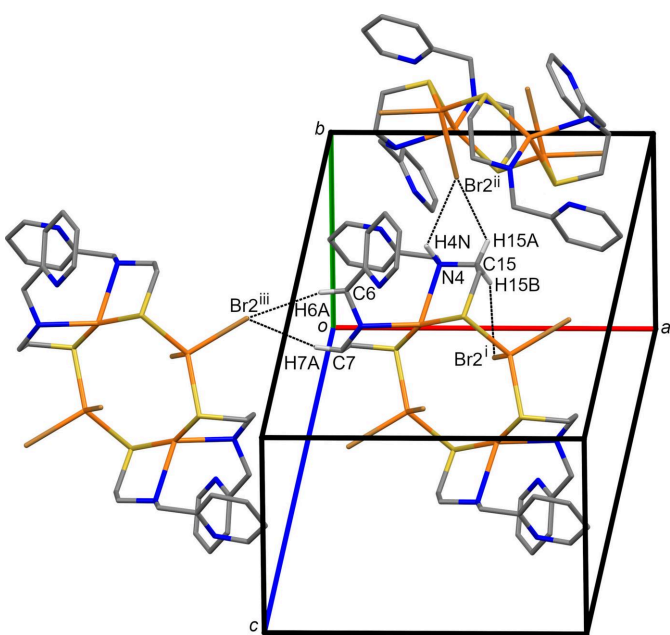
$D - H \cdots A$	$D - H$	$H \cdots A$	$D \cdots A$	$D - H \cdots A$
N4—H4N···Br2 ⁱⁱ	1.00	2.95	3.572 (3)	121
C6—H6A···Br1 ⁱⁱⁱ	0.99	3.02	3.944 (4)	157
C7—H7A···Br1 ⁱⁱⁱ	0.99	3.02	3.978 (4)	163
C15—H15A···Br2 ⁱⁱ	0.99	2.86	3.503 (4)	123
C15—H15B···Br2 ⁱ	0.99	3.09	3.973 (4)	149

Symmetry codes: (i) $-x + 1, -y + 1, -z + 1$; (ii) $x, -y + \frac{3}{2}, z - \frac{1}{2}$; (iii) $-x, -y + 1, -z + 1$.

hydrogen bonding (Fig. 3 and Table 3). The pendant pyridyl rings (centroids *Cg1*: N1/C1–C5; *Cg2*: N3/C9–C13) participate in a fourfold aryl embrace around a crystallographic inversion center with centroid–centroid distances of 4.453 (2) and 4.873 (2) \AA (Table 2). The pyridyl planes subtend an angle of 62.87 (13) $^\circ$. Most of the hydrogen bonds involve C—H donors and Br acceptors (Brammer *et al.*, 2001). Neither nitrogen atom of the pendant pyridyl rings participates in intermolecular hydrogen bonding.

**Figure 2**

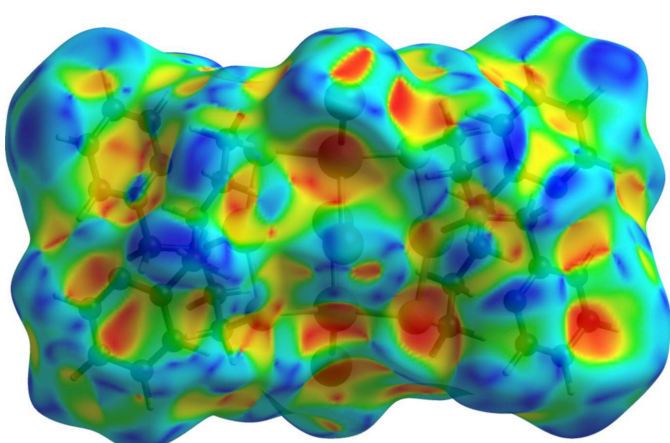
Fourfold aryl embrace between two pairs of inversion-related molecules of **1** viewed down the *a* axis illustrated using *Mercury* (Macrae *et al.*, 2020). Hydrogen atoms were omitted for clarity. Ring centroids are shown as red spheres. Cyan dashed lines show centroid–centroid distances (for additional numerical data, see Table 2).

**Figure 3**

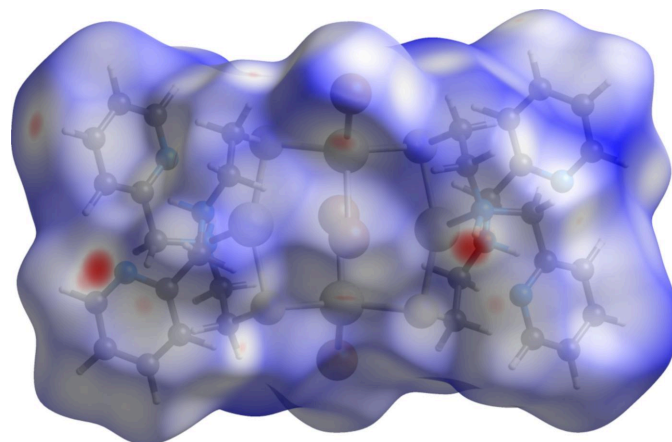
A view of N—H···Br and C—H···Br hydrogen bonds in compound **1** shown as dashed lines illustrated using *Mercury* (Macrae *et al.*, 2020). Symmetry codes as in Table 3.

4. Hirshfeld surface analysis

Intermolecular interactions were investigated by quantitative analysis of the Hirshfeld surface and visualized with *Crystal-Explorer* 21.5 (Spackman *et al.*, 2021). The Hirshfeld surface of **1** plotted over shape-index did not have the hourglass figures associated with face-to-face aromatic interactions (Fig. 4). Instead, circular and wedge-shaped blue bumps associated with N3 as the edge of the pyridyl ring (top right) complement a pair of similarly shaped red pits on the face of the N1 pyridyl ring (lower right). The reverse side of the N1 pyridyl ring (upper left) has a multicolored iris-like feature and a large

**Figure 4**

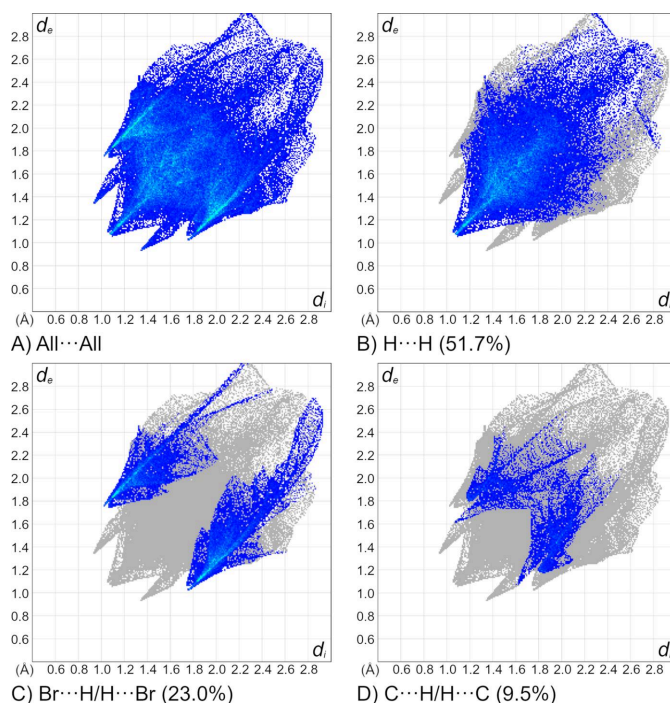
Hirshfeld surface of **1** plotted over shape-index generated with *Crystal-Explorer* 21.5 (Spackman *et al.*, 2021). Blue and red areas represent bumps and hollow regions, respectively, on the shape-index surface.

**Figure 5**

Hirshfeld surface of **1** plotted over normalized contact distance (d_{norm}) in the range from -0.2689 (red) to 1.5908 (blue) a.u. generated with *CrystalExplorer21.5* (Spackman *et al.*, 2021).

blue bump while complementary characteristics lie across the center of the molecule. A feature reminiscent of a paw print with red digital pad pits extending over the reverse face of the N3 pyridyl ring and a blue metacarpal pad bump over the attached methylene (lower left) complements a reverse-colored paw print overlying the inner edge of the N1 pyridyl ring.

The Hirshfeld surface of **1** mapped with the function d_{norm} , the sum of the distances from a surface point to the nearest

**Figure 6**

The full two-dimensional fingerprint plots for **1**, showing (a) all interactions, and components delineated into (b) $\text{H}\cdots\text{H}$, (c) $\text{Br}\cdots\text{H}/\text{H}\cdots\text{Br}$ and (d) $\text{C}\cdots\text{H}/\text{H}\cdots\text{C}$ interactions generated with *CrystalExplorer 21.5* (Spackman *et al.*, 2021). The d_i and d_e values are closest internal and external distances (in Å) from given points on the Hirshfeld surface.

interior (d_i) and exterior (d_e) atoms normalized by the van der Waals (vdW) radii of the corresponding atom (rvdW), is shown in Fig. 5. Contacts near and longer than the sum of van der Waals radii are shown in white and blue, respectively. Red areas are observed for atoms associated with close contacts at least 0.050 Å shorter than the sum of van der Waals radii (Bondi, 1964). The most intense red spots correspond to an intermolecular contact between H_2N and adjacent atoms N3 and C9. Neighboring pale-red regions reflect a contact between N1 and C13, respectively. Medium intensity red spots are associated with Br1 and H3.

The overall 2D fingerprint plot for **1** is provided in Fig. 6a while the interactions delineated into $\text{H}\cdots\text{H}$ (51.7%), $\text{Br}\cdots\text{H}/\text{H}\cdots\text{Br}$ (23.0%), and $\text{C}\cdots\text{H}/\text{H}\cdots\text{C}$ (9.5%) contacts are shown in Fig. 6b–d. Other minor contributions to the Hirshfeld surface are from $\text{S}\cdots\text{H}/\text{H}\cdots\text{S}$ (7.5%), $\text{N}\cdots\text{H}/\text{H}\cdots\text{N}$ (4.7%), $\text{N}\cdots\text{C/C}\cdots\text{N}$ (1.8%), $\text{Hg}\cdots\text{H}/\text{H}\cdots\text{Hg}$ (1.4%), $\text{Br}\cdots\text{C/C}\cdots\text{Br}$ (0.3%), $\text{N}\cdots\text{N}$ (0.1%), and $\text{C}\cdots\text{C}$ (0.1%) interactions.

5. Database survey

A search of the Cambridge Structural Database (CSD, Version 5.44, update of April 2023; Groom *et al.*, 2016) using *ConQuest* (Bruno *et al.*, 2002) for metal complexes of **L** yielded 21 hits. Most of the complexes feature an N,N' - μ_2 -S binding mode for **L** including $[\text{PdL}]_4\text{Cl}(\text{ClO}_4)_3\cdot\text{CH}_3\text{OH}\cdot\text{H}_2\text{O}$ (refcode SUZDUM; Kawahashi *et al.*, 2001), which had a Pd_4S_4 metallocycle with boat conformation. Salts of group 12 metal ions with weakly coordinating perchlorate and tetrafluoroborate counter-ions have generated a variety of solvated complex ions with composition $[\text{Zn}_3\text{L}_4]^{2+}$ (refcode BITNIB; Mikuriya *et al.*, 1998; JEHWEB: Hallinger *et al.*, 2017; ZACWAB; Brand & Vahrenkamp, 1995) and $[\text{HgZn}_2\text{L}_4]^{2+}$ (refcodes JEHWIF, JEHWOL, JEHWUR, JEHXAY, JEHXEC; Hallinger *et al.*, 2017). Additional complexes of tridentate **L** with group 12 metal ions include $[\text{Hg}_5\text{L}_6](\text{ClO}_4)_4\cdot\text{toluene}$ (DABJIB; Viehweg *et al.*, 2010), $[\text{ZnLCl}]_n$ (ZACWEF; Brand & Vahrenkamp, 1995), $[\text{ZnL}(\text{acetato}-\text{O})]_2$ (ZACWIJ; Brand & Vahrenkamp, 1995), and $[\text{ZnL}(\text{quinoline}-2\text{-carboxylato}-\text{N},\text{O})]$ (ZACWUV; Brand & Vahrenkamp, 1995). The only complexes of **L** with pendant pyridyl rings are $[\text{MoL}(\text{S}_2)_2\text{O}]$ (refcode OTUHER; Wei *et al.*, 2011), $[\text{ZnL}_2]$ (refcode ZACWOP; Brand & Vahrenkamp, 1995) and $[\text{CuL}]_4$ (refcode TEVMAI; Stange *et al.*, 1996).

A search of the Cambridge Structural Database (CSD, Version 5.44, update of April 2023; (Groom *et al.*, 2016) using *ConQuest* (Bruno *et al.*, 2002) for Hg_4S_4 metallacycles yielded eight tetramercury hits. Complexes with chelating N and S donor aminoethanethiolate ligands share an extended chair conformation comparable to **1** with varying degrees of back-folding (refcode IKUVUH: Clegg, 2016; refcodes DENKUD and DENLEO: Bharara *et al.*, 2006a; refcode ECIYOF: Bharara *et al.*, 2006b; refcode JIZWEU: Casals *et al.*, 1991). Complexes with separate pyridyl and alkylthiolate ligands exhibit nearly planar Hg_4S_4 rings cinched across the middle by a pair of μ -Cl ligands (refcode BTCHGP: Carty, *et al.*, 1978; refcode TBTPHG: Carty, *et al.*, 1979). In contrast, a chair ring

Table 4
Experimental details.

Crystal data	
Chemical formula	[Hg ₄ Br ₄ (C ₈ H ₁₁ N ₂ S) ₄]
M _r	1790.99
Crystal system, space group	Monoclinic, P ₂ /c
Temperature (K)	100
<i>a</i> , <i>b</i> , <i>c</i> (Å)	12.3055 (8), 12.1464 (8), 14.9763 (9)
β (°)	99.509 (1)
<i>V</i> (Å ³)	2207.7 (2)
<i>Z</i>	2
Radiation type	Mo <i>K</i> α
μ (mm ⁻¹)	17.71
Crystal size (mm)	0.35 × 0.31 × 0.22
Data collection	
Diffractometer	Bruker SMART APEXII CCD
Absorption correction	Numerical (<i>SADABS</i> ; Krause <i>et al.</i> , 2015)
<i>T</i> _{min} , <i>T</i> _{max}	0.024, 0.114
No. of measured, independent and observed [<i>I</i> > 2σ(<i>I</i>)] reflections	32818, 4414, 4133
<i>R</i> _{int}	0.027
(sin θ/λ) _{max} (Å ⁻¹)	0.621
Refinement	
<i>R</i> [<i>F</i> ² > 2σ(<i>F</i> ²)], <i>wR</i> (<i>F</i> ²), <i>S</i>	0.016, 0.034, 1.18
No. of reflections	4414
No. of parameters	235
H-atom treatment	H-atom parameters constrained
Δρ _{max} , Δρ _{min} (e Å ⁻³)	0.96, -0.73

Computer programs: *APEX3* (Bruker, 2015), *SAINT-Plus* (Bruker, 2012), *SHELXT2014/5* (Sheldrick, 2015a), *SHELXL2014/5* (Sheldrick, 2015b), *ShelXle* (Hübschle *et al.*, 2011), *ORTEP-3* for Windows (Farrugia, 2012), *Mercury* (Macrae *et al.*, 2020), *CrystalExplorer21.5* (Spackman *et al.*, 2021), *OLEX2* (Dolomanov *et al.*, 2009) and *publCIF* (Westrip, 2010).

conformation with only four coplanar atoms and μ-Cl was observed with dipropyldithiocarbamate ligands (XOKPAR: Loseva *et al.*, 2019).

6. Synthesis and crystallization

A solution of HgBr₂ (942 mg, 2.61 mmol) in 15 mL methanol was added to a stirred solution of **LH** (445 mg, 2.64 mmol) and NaOH (104 mg, 2.60 mmol) in 20 mL methanol. A white precipitate characterized as **1** was collected by vacuum filtration and dried overnight under vacuum (971 mg, 542 μmol, 83% yield). X-ray quality colorless plates were formed by dissolving the precipitate in a minimum amount of hot acetonitrile and setting aside for slow evaporation. M.p. 438 K (dec). ¹H NMR (saturated, CD₃CN): 8.514 (*d*, 1H, *J* = 5.0), 7.802 (*ddd*, 1H, *J* = 1.7, 7.6, 7.6), 7.373 (*dd*, 1H, *J* = 5.0, 7.9), 4.144 (*d*, 2H, *J* = 4.1), 2.928 (*bm*, 1H), 2.804 (*m*, 1H) 2.668 (*m*, 1H). Analysis calculated for C₃₂H₄₄Br₄Hg₄N₈S₄: C, 21.46; H, 2.48; N, 6.26. Found: C, 21.35; H, 2.45; N, 6.12.

7. Refinement

Crystal data, data collection and structure refinement details are summarized in Table 4. The hydrogen atoms were placed in calculated positions with C–H distances of 0.95 (aromatic) and 0.99 Å (methylene) and refined as riding atoms with *U*_{iso}(H) = 1.2*U*_{eq}(C).Å

Acknowledgements

The authors thank William & Mary's Swem Library for organizing a Faculty Writer's Retreat at which this manuscript was completed and for providing open-access financial assistance.

Funding information

Funding for this research was provided by: William & Mary.

References

- Akhtar, M., Tahir, M. N., Saleem, M., Mazhar, M., Rauf, A., Isab, A. A., Ahmad, S. & Nadeem, S. (2015). *Russ. J. Inorg. Chem.* **60**, 1568–1572.
- Avdeef, A., Hartenstein, F., Chemotti, A. R. J. & Brown, J. A. (1992). *Inorg. Chem.* **31**, 3701–3705.
- Bharara, M. S., Parkin, S. & Atwood, D. A. (2006a). *Inorg. Chem.* **45**, 7261–7268.
- Bharara, M. S., Parkin, S. & Atwood, D. A. (2006b). *Inorg. Chem.* **45**, 2112–2118.
- Bondi, A. (1964). *J. Phys. Chem.* **68**, 441–451.
- Brammer, L., Bruton, E. A. & Sherwood, P. (2001). *Cryst. Growth Des.* **1**, 277–290.
- Brand, U. & Vahrenkamp, H. (1995). *Inorg. Chem.* **34**, 3285–3293.
- Brennan, H. M., Bunde, S. G., Kuang, Q., Palomino, T. V., Sacks, J. S., Berry, S. M., Butcher, R. J., Poutsma, J. C., Pike, R. D. & Bebout, D. C. (2022). *Inorg. Chem.* **61**, 19857–19869.
- Bruker (2012). *SAINT-Plus*. Bruker AXS Inc. Madison, Wisconsin, USA.
- Bruker (2015). *APEX3*. Bruker AXS Inc. Madison, Wisconsin, USA
- Bruno, I. J., Cole, J. C., Edgington, P. R., Kessler, M., Macrae, C. F., McCabe, P., Pearson, J. & Taylor, R. (2002). *Acta Cryst. B* **58**, 389–397.
- Canty, A. J., Raston, C. L. & White, A. H. (1978). *Aust. J. Chem.* **31**, 677–684.
- Canty, A. J., Raston, C. L. & White, A. H. (1979). *Aust. J. Chem.* **32**, 1165–1166.
- Casals, I., González-Duarte, P., Clegg, W., Foces-Foces, C., Cano, F. H., Martínez-Ripoll, M., Gómez, M. & Solans, X. (1991). *J. Chem. Soc. Dalton Trans.* pp. 2511–2518.
- Clegg, W. (2016). *CSD communication* (refcode IKUVUH). CCDC, Cambridge, England.
- Dolomanov, O. V., Bourhis, L. J., Gildea, R. J., Howard, J. A. K. & Puschmann, H. (2009). *J. Appl. Cryst.* **42**, 339–341.
- Farrugia, L. J. (2012). *J. Appl. Cryst.* **45**, 849–854.
- Fawcett, T. G., Ou, C., Potenza, J. A. & Schugar, H. J. (1978). *J. Am. Chem. Soc.* **100**, 2058–2062.
- Fleischer, H., Hardt, S. & Schollmeyer, D. (2006). *Inorg. Chem.* **45**, 8318–8325.
- Groom, C. R., Bruno, I. J., Lightfoot, M. P. & Ward, S. C. (2016). *Acta Cryst. B* **72**, 171–179.
- Hallinger, M. R., Gerhard, A. C., Ritz, M. D., Sacks, J. S., Poutsma, J. C., Pike, R. D., Wojtas, L. & Bebout, D. C. (2017). *ACS Omega*, **2**, 6391–6404.
- Hu, L., Fang, J., Zhang, X., Li, M. & Li, S. (2020). *Russ. J. Inorg. Chem.* **65**, 1718–1725.
- Hübschle, C. B., Sheldrick, G. M. & Dittrich, B. (2011). *J. Appl. Cryst.* **44**, 1281–1284.
- Kaptein, B., Wang-Griffin, L., Barf, G. & Kellogg, R. M. (1987). *J. Chem. Soc. Chem. Commun.* pp. 1457–1459.
- Kawahashi, T., Mikuriya, M., Nukada, R. & Lim, J. (2001). *Bull. Chem. Soc. Jpn.* **74**, 323–329.
- Krause, L., Herbst-Irmer, R., Sheldrick, G. M. & Stalke, D. (2015). *J. Appl. Cryst.* **48**, 3–10.

- Lai, W., Berry, S. M., Kaplan, W. P., Hain, M. S., Poutsma, J. C., Butcher, R. J., Pike, R. D. & Bebout, D. C. (2013). *Inorg. Chem.* **52**, 2286–2288.
- Loseva, O. V., Rodina, T. A., Ivanov, A. V., Smolentsev, A. I. & Antzutkin, O. N. (2019). *Russ. Chem. Bull.* **68**, 782–792.
- Macrae, C. F., Sovago, I., Cottrell, S. J., Galek, P. T. A., McCabe, P., Pidcock, E., Platings, M., Shields, G. P., Stevens, J. S., Towler, M. & Wood, P. A. (2020). *J. Appl. Cryst.* **53**, 226–235.
- Mikuriya, M., Jian, X., Ikemi, S., Kawahashi, T. & Tsutsumi, H. (1998). *Bull. Chem. Soc. Jpn.* **71**, 2161–2168.
- Ritz, M. D., Gerhard, A. C., Pike, R. D. & Bebout, D. C. (2019). *Eur. J. Inorg. Chem.* pp. 4070–4077.
- Sheldrick, G. M. (2015a). *Acta Cryst. A* **71**, 3–8.
- Sheldrick, G. M. (2015b). *Acta Cryst. C* **71**, 3–8.
- Spackman, P. R., Turner, M. J., McKinnon, J. J., Wolff, S. K., Grimwood, D. J., Jayatilaka, D. & Spackman, M. A. (2021). *J. Appl. Cryst.* **54**, 1006–1011.
- Stange, A. F., Klinkhammer, K. W. & Kaim, W. (1996). *Inorg. Chem.* **35**, 4087–4089.
- Tuntulani, T., Reibenspies, J. H., Farmer, P. J. & Darensbourg, M. Y. (1992). *Inorg. Chem.* **31**, 3497–3499.
- Viehweg, J. A., Stamps, S. M., Dertinger, J. J., Green, R. L., Harris, K. E., Butcher, R. J., Andriole, E. J., Poutsma, J. C., Berry, S. M. & Bebout, D. C. (2010). *Dalton Trans.* **39**, 3174–3176.
- Wei, Z., Long, L., Wei, J. & Liu, X. (2011). *Inorg. Chim. Acta*, **375**, 320–323.
- Westrip, S. P. (2010). *J. Appl. Cryst.* **43**, 920–925.

supporting information

Acta Cryst. (2023). E79, 952–957 [https://doi.org/10.1107/S205698902300823X]

Crystal structure and Hirshfeld surface analysis of *cyclo*-tetrabromido- $1\kappa^2Br,3\kappa^2Br$ -tetrakis(μ_2 -2-{{[(pyridin-2-yl)methyl]amino}ethane-1-thiolato- $\kappa^3N,S:S$)tetramercury(II)

Isla D. Thomas, Kathryn R. Kocher, Julie A. Viehweg, Robert D. Pike and Deborah C. Bebout

Computing details

Data collection: *APEX3* (Bruker, 2015); cell refinement: *SAINT-Plus* (Bruker, 2012); data reduction: *SAINT-Plus* (Bruker, 2012); program(s) used to solve structure: *SHELXT2014/5* (Sheldrick, 2015a); program(s) used to refine structure: *SHELXL2014/5* (Sheldrick, 2015b); molecular graphics: *ShelXle* (Hübschle *et al.*, 2011); software used to prepare material for publication: *ORTEP-3 for Windows* (Farrugia, 2012), *Mercury* 2022.3.0 (Macrae *et al.*, 2020), *CrystalExplorer21.5* (Spackman *et al.*, 2021), *OLEX2* (Dolomanov *et al.*, 2009) and *publCIF* (Westrip, 2010).

cyclo-Tetrabromido- $1\kappa^2Br,3\kappa^2Br$ -tetrakis(μ_2 -2-{{[(pyridin-2-yl)methyl]amino}ethane-1-thiolato- $\kappa^3N,S:S$)tetramercury(II)

Crystal data

[Hg ₄ Br ₄ (C ₈ H ₁₁ N ₂ S) ₄]	F(000) = 1632
M _r = 1790.99	D _x = 2.694 Mg m ⁻³
Monoclinic, P2 ₁ /c	Mo K α radiation, λ = 0.71073 Å
<i>a</i> = 12.3055 (8) Å	Cell parameters from 9997 reflections
<i>b</i> = 12.1464 (8) Å	θ = 2.2–26.2°
<i>c</i> = 14.9763 (9) Å	μ = 17.71 mm ⁻¹
β = 99.509 (1)°	<i>T</i> = 100 K
<i>V</i> = 2207.7 (2) Å ³	Block, colourless
Z = 2	0.35 × 0.31 × 0.22 mm

Data collection

Bruker SMART APEXII CCD	4414 independent reflections
diffractometer	4133 reflections with $I > 2\sigma(I)$
Radiation source: fine-focus sealed tube	$R_{\text{int}} = 0.027$
φ and ω scans	$\theta_{\text{max}} = 26.2^\circ$, $\theta_{\text{min}} = 1.7^\circ$
Absorption correction: numerical	$h = -15 \rightarrow 15$
(SADABS; Krause <i>et al.</i> , 2015)	$k = -15 \rightarrow 15$
$T_{\text{min}} = 0.024$, $T_{\text{max}} = 0.114$	$l = -18 \rightarrow 18$
32818 measured reflections	

Refinement

Refinement on F^2	4414 reflections
Least-squares matrix: full	235 parameters
$R[F^2 > 2\sigma(F^2)] = 0.016$	0 restraints
$wR(F^2) = 0.034$	Primary atom site location: other
$S = 1.18$	

Hydrogen site location: inferred from
neighbouring sites
H-atom parameters constrained

$$w = 1/[\sigma^2(F_o^2) + (0.0066P)^2 + 5.3501P]$$

$$\text{where } P = (F_o^2 + 2F_c^2)/3$$

$$(\Delta/\sigma)_{\max} = 0.003$$

$$\Delta\rho_{\max} = 0.96 \text{ e \AA}^{-3}$$

$$\Delta\rho_{\min} = -0.73 \text{ e \AA}^{-3}$$

Special details

Geometry. All esds (except the esd in the dihedral angle between two l.s. planes) are estimated using the full covariance matrix. The cell esds are taken into account individually in the estimation of esds in distances, angles and torsion angles; correlations between esds in cell parameters are only used when they are defined by crystal symmetry. An approximate (isotropic) treatment of cell esds is used for estimating esds involving l.s. planes.

Fractional atomic coordinates and isotropic or equivalent isotropic displacement parameters (\AA^2)

	<i>x</i>	<i>y</i>	<i>z</i>	$U_{\text{iso}}^*/U_{\text{eq}}$
Hg1	0.36010 (2)	0.63859 (2)	0.39709 (2)	0.01596 (4)
Hg2	0.34257 (2)	0.36960 (2)	0.51023 (2)	0.01555 (4)
Br1	0.17236 (3)	0.28583 (3)	0.57228 (2)	0.01937 (8)
Br2	0.41406 (3)	0.54687 (3)	0.61405 (2)	0.01797 (8)
S1	0.27476 (7)	0.45682 (7)	0.36173 (6)	0.01507 (17)
S2	0.50720 (7)	0.76760 (7)	0.45273 (6)	0.01603 (18)
N1	0.2436 (3)	0.8986 (3)	0.4380 (2)	0.0259 (7)
N2	0.1844 (2)	0.6839 (2)	0.4320 (2)	0.0187 (6)
H2N	0.196666	0.724631	0.490813	0.028*
N3	0.1801 (3)	0.7126 (2)	0.1325 (2)	0.0197 (7)
N4	0.3891 (2)	0.7134 (2)	0.2473 (2)	0.0158 (6)
H4N	0.344787	0.782017	0.232890	0.024*
C1	0.2971 (4)	0.9946 (3)	0.4380 (3)	0.0297 (9)
H1	0.341373	1.017980	0.492738	0.036*
C2	0.2913 (3)	1.0613 (3)	0.3629 (3)	0.0270 (9)
H2	0.329526	1.129507	0.366415	0.032*
C3	0.2293 (4)	1.0275 (3)	0.2829 (3)	0.0301 (10)
H3	0.224540	1.071203	0.229798	0.036*
C4	0.1736 (3)	0.9277 (3)	0.2815 (3)	0.0256 (9)
H4	0.129535	0.902190	0.227357	0.031*
C5	0.1833 (3)	0.8660 (3)	0.3604 (3)	0.0182 (8)
C6	0.1227 (3)	0.7578 (3)	0.3633 (3)	0.0206 (8)
H6A	0.048433	0.771744	0.378057	0.025*
H6B	0.113785	0.722092	0.303082	0.025*
C7	0.1260 (3)	0.5811 (3)	0.4463 (3)	0.0183 (8)
H7A	0.047349	0.597985	0.446802	0.022*
H7B	0.157278	0.550215	0.506197	0.022*
C8	0.1341 (3)	0.4954 (3)	0.3737 (2)	0.0184 (8)
H8A	0.096082	0.524139	0.314866	0.022*
H8B	0.094329	0.428402	0.387721	0.022*
C9	0.0708 (3)	0.7033 (3)	0.1080 (3)	0.0215 (8)
H9	0.029095	0.769155	0.096668	0.026*
C10	0.0147 (3)	0.6047 (3)	0.0980 (3)	0.0231 (8)
H10	-0.063114	0.602404	0.080596	0.028*

C11	0.0758 (3)	0.5094 (3)	0.1142 (2)	0.0221 (8)
H11	0.040555	0.439620	0.107402	0.026*
C12	0.1888 (3)	0.5162 (3)	0.1405 (2)	0.0192 (8)
H12	0.232040	0.451499	0.152687	0.023*
C13	0.2376 (3)	0.6192 (3)	0.1487 (2)	0.0164 (7)
C14	0.3616 (3)	0.6329 (3)	0.1735 (2)	0.0196 (8)
H14A	0.395562	0.560988	0.192635	0.024*
H14B	0.391918	0.658056	0.119720	0.024*
C15	0.5074 (3)	0.7401 (3)	0.2651 (2)	0.0175 (7)
H15A	0.529249	0.772789	0.210122	0.021*
H15B	0.550610	0.671881	0.279782	0.021*
C16	0.5324 (3)	0.8206 (3)	0.3433 (2)	0.0192 (8)
H16A	0.486953	0.887453	0.328254	0.023*
H16B	0.610658	0.842917	0.349405	0.023*

Atomic displacement parameters (\AA^2)

	U^{11}	U^{22}	U^{33}	U^{12}	U^{13}	U^{23}
Hg1	0.01171 (7)	0.01497 (7)	0.02108 (8)	-0.00221 (5)	0.00233 (5)	0.00253 (5)
Hg2	0.01402 (7)	0.01313 (7)	0.01822 (7)	-0.00079 (5)	-0.00112 (5)	0.00195 (5)
Br1	0.01458 (16)	0.01840 (18)	0.02510 (19)	-0.00292 (13)	0.00323 (14)	0.00137 (15)
Br2	0.01992 (17)	0.01448 (17)	0.01915 (18)	-0.00256 (14)	0.00219 (14)	-0.00390 (14)
S1	0.0154 (4)	0.0135 (4)	0.0154 (4)	-0.0004 (3)	0.0002 (3)	0.0004 (3)
S2	0.0140 (4)	0.0129 (4)	0.0204 (5)	-0.0002 (3)	0.0008 (3)	-0.0012 (3)
N1	0.0307 (19)	0.0229 (17)	0.0250 (18)	-0.0046 (15)	0.0073 (15)	0.0007 (14)
N2	0.0165 (15)	0.0159 (15)	0.0244 (17)	0.0005 (12)	0.0055 (13)	-0.0004 (13)
N3	0.0197 (16)	0.0178 (16)	0.0211 (16)	0.0022 (13)	0.0016 (13)	-0.0018 (13)
N4	0.0136 (14)	0.0146 (15)	0.0191 (15)	0.0004 (12)	0.0019 (12)	0.0008 (12)
C1	0.035 (2)	0.026 (2)	0.028 (2)	-0.0085 (18)	0.0036 (19)	-0.0003 (18)
C2	0.030 (2)	0.021 (2)	0.033 (2)	-0.0052 (17)	0.0117 (19)	-0.0024 (17)
C3	0.042 (3)	0.023 (2)	0.029 (2)	0.0056 (18)	0.014 (2)	0.0066 (18)
C4	0.034 (2)	0.020 (2)	0.022 (2)	0.0045 (17)	0.0018 (18)	-0.0015 (16)
C5	0.0160 (17)	0.0160 (18)	0.024 (2)	0.0057 (14)	0.0082 (15)	-0.0016 (15)
C6	0.0155 (17)	0.0208 (19)	0.025 (2)	0.0008 (15)	0.0022 (15)	0.0011 (16)
C7	0.0130 (17)	0.0193 (19)	0.0237 (19)	0.0008 (14)	0.0061 (15)	0.0046 (16)
C8	0.0140 (17)	0.0170 (18)	0.0223 (19)	-0.0032 (14)	-0.0029 (15)	0.0044 (15)
C9	0.0198 (19)	0.021 (2)	0.024 (2)	0.0047 (15)	0.0039 (16)	0.0014 (16)
C10	0.0178 (19)	0.031 (2)	0.0194 (19)	-0.0020 (16)	-0.0010 (15)	-0.0008 (17)
C11	0.025 (2)	0.0187 (19)	0.022 (2)	-0.0064 (16)	0.0012 (16)	0.0016 (16)
C12	0.0233 (19)	0.0178 (18)	0.0162 (18)	0.0021 (15)	0.0024 (15)	0.0027 (15)
C13	0.0187 (18)	0.0174 (18)	0.0130 (17)	0.0024 (14)	0.0022 (14)	-0.0004 (14)
C14	0.0195 (18)	0.0191 (19)	0.0198 (19)	0.0025 (15)	0.0021 (15)	-0.0037 (15)
C15	0.0139 (17)	0.0196 (18)	0.0186 (18)	0.0006 (14)	0.0015 (14)	0.0078 (15)
C16	0.0149 (17)	0.0159 (18)	0.025 (2)	-0.0015 (14)	-0.0011 (15)	0.0082 (15)

Geometric parameters (\AA , $^{\circ}$)

Hg1—N2	2.372 (3)	C4—C5	1.387 (5)
Hg1—N4	2.500 (3)	C4—H4	0.9500
Hg1—S1	2.4646 (9)	C5—C6	1.515 (5)
Hg1—S2	2.4348 (9)	C6—H6A	0.9900
Hg2—S1	2.4802 (9)	C6—H6B	0.9900
Hg2—S2 ⁱ	2.4826 (9)	C7—C8	1.520 (5)
Hg2—Br1	2.6323 (4)	C7—H7A	0.9900
Hg2—Br2	2.7158 (4)	C7—H7B	0.9900
S1—C8	1.831 (4)	C8—H8A	0.9900
S2—C16	1.835 (4)	C8—H8B	0.9900
N1—C5	1.332 (5)	C9—C10	1.378 (5)
N1—C1	1.338 (5)	C9—H9	0.9500
N2—C7	1.473 (4)	C10—C11	1.380 (5)
N2—C6	1.478 (5)	C10—H10	0.9500
N2—H2N	1.0000	C11—C12	1.384 (5)
N3—C13	1.338 (5)	C11—H11	0.9500
N3—C9	1.340 (5)	C12—C13	1.384 (5)
N4—C15	1.472 (4)	C12—H12	0.9500
N4—C14	1.473 (4)	C13—C14	1.518 (5)
N4—H4N	1.0000	C14—H14A	0.9900
C1—C2	1.379 (6)	C14—H14B	0.9900
C1—H1	0.9500	C15—C16	1.518 (5)
C2—C3	1.372 (6)	C15—H15A	0.9900
C2—H2	0.9500	C15—H15B	0.9900
C3—C4	1.391 (6)	C16—H16A	0.9900
C3—H3	0.9500	C16—H16B	0.9900
N2—Hg1—N4	112.59 (10)	N2—C6—H6B	109.6
N2—Hg1—S2	115.39 (8)	C5—C6—H6B	109.6
N4—Hg1—S1	104.57 (7)	H6A—C6—H6B	108.1
N4—Hg1—S2	82.25 (7)	N2—C7—C8	112.6 (3)
S1—Hg1—S2	156.40 (3)	N2—C7—H7A	109.1
Hg1—S1—Hg2	96.99 (3)	C8—C7—H7A	109.1
Hg1—S2—Hg2 ⁱ	97.38 (3)	N2—C7—H7B	109.1
S1—Hg2—S2 ⁱ	127.94 (3)	C8—C7—H7B	109.1
S1—Hg2—Br1	108.19 (2)	H7A—C7—H7B	107.8
S1—Hg2—Br2	101.76 (2)	C7—C8—S1	114.8 (2)
S2 ⁱ —Hg2—Br1	105.56 (2)	C7—C8—H8A	108.6
S2 ⁱ —Hg2—Br2	104.21 (2)	S1—C8—H8A	108.6
Br1—Hg2—Br2	107.804 (12)	C7—C8—H8B	108.6
C8—S1—Hg1	97.22 (12)	S1—C8—H8B	108.6
C8—S1—Hg2	101.84 (12)	H8A—C8—H8B	107.5
C16—S2—Hg1	98.39 (12)	N3—C9—C10	124.4 (4)
C16—S2—Hg2 ⁱ	101.88 (12)	N3—C9—H9	117.8
C5—N1—C1	117.6 (3)	C10—C9—H9	117.8
C7—N2—C6	114.2 (3)	C9—C10—C11	117.5 (3)

C7—N2—Hg1	108.7 (2)	C9—C10—H10	121.3
C6—N2—Hg1	111.7 (2)	C11—C10—H10	121.3
C7—N2—H2N	107.3	C10—C11—C12	119.5 (3)
C6—N2—H2N	107.3	C10—C11—H11	120.2
Hg1—N2—H2N	107.3	C12—C11—H11	120.2
C13—N3—C9	117.1 (3)	C11—C12—C13	118.7 (3)
C15—N4—C14	112.4 (3)	C11—C12—H12	120.6
C15—N4—Hg1	101.6 (2)	C13—C12—H12	120.6
C14—N4—Hg1	112.5 (2)	N3—C13—C12	122.8 (3)
C15—N4—H4N	110.0	N3—C13—C14	115.6 (3)
C14—N4—H4N	110.0	C12—C13—C14	121.6 (3)
Hg1—N4—H4N	110.0	N4—C14—C13	110.7 (3)
N1—C1—C2	123.5 (4)	N4—C14—H14A	109.5
N1—C1—H1	118.2	C13—C14—H14A	109.5
C2—C1—H1	118.2	N4—C14—H14B	109.5
C3—C2—C1	118.9 (4)	C13—C14—H14B	109.5
C3—C2—H2	120.6	H14A—C14—H14B	108.1
C1—C2—H2	120.6	N4—C15—C16	110.5 (3)
C2—C3—C4	118.4 (4)	N4—C15—H15A	109.5
C2—C3—H3	120.8	C16—C15—H15A	109.5
C4—C3—H3	120.8	N4—C15—H15B	109.5
C5—C4—C3	119.0 (4)	C16—C15—H15B	109.5
C5—C4—H4	120.5	H15A—C15—H15B	108.1
C3—C4—H4	120.5	C15—C16—S2	114.9 (2)
N1—C5—C4	122.6 (4)	C15—C16—H16A	108.6
N1—C5—C6	116.1 (3)	S2—C16—H16A	108.6
C4—C5—C6	121.3 (3)	C15—C16—H16B	108.6
N2—C6—C5	110.4 (3)	S2—C16—H16B	108.6
N2—C6—H6A	109.6	H16A—C16—H16B	107.5
C5—C6—H6A	109.6		
C5—N1—C1—C2	1.1 (6)	C13—N3—C9—C10	-0.4 (6)
N1—C1—C2—C3	-1.3 (7)	N3—C9—C10—C11	-0.2 (6)
C1—C2—C3—C4	0.9 (6)	C9—C10—C11—C12	0.8 (6)
C2—C3—C4—C5	-0.5 (6)	C10—C11—C12—C13	-0.8 (5)
C1—N1—C5—C4	-0.6 (6)	C9—N3—C13—C12	0.3 (5)
C1—N1—C5—C6	-179.2 (3)	C9—N3—C13—C14	178.2 (3)
C3—C4—C5—N1	0.3 (6)	C11—C12—C13—N3	0.2 (5)
C3—C4—C5—C6	178.8 (3)	C11—C12—C13—C14	-177.5 (3)
C7—N2—C6—C5	173.9 (3)	C15—N4—C14—C13	-172.3 (3)
Hg1—N2—C6—C5	-62.3 (3)	Hg1—N4—C14—C13	73.7 (3)
N1—C5—C6—N2	-30.2 (4)	N3—C13—C14—N4	51.0 (4)
C4—C5—C6—N2	151.3 (3)	C12—C13—C14—N4	-131.1 (3)
C6—N2—C7—C8	79.5 (4)	C14—N4—C15—C16	-178.4 (3)
Hg1—N2—C7—C8	-45.8 (3)	Hg1—N4—C15—C16	-57.9 (3)
N2—C7—C8—S1	57.4 (4)	N4—C15—C16—S2	64.1 (3)

Hg1—S1—C8—C7	−34.3 (3)	Hg1—S2—C16—C15	−29.0 (3)
Hg2—S1—C8—C7	64.5 (3)	Hg2 ⁱ —S2—C16—C15	70.4 (3)

Symmetry code: (i) $-x+1, -y+1, -z+1$.

Hydrogen-bond geometry (\AA , °)

$D\cdots H$	$D\cdots A$	$H\cdots A$	$D\cdots A$	$D\cdots H\cdots A$
N2—H2N \cdots N3 ⁱⁱ	1.00	2.30	3.264 (4)	163
N4—H4N \cdots Br2 ⁱⁱⁱ	1.00	2.95	3.572 (3)	121
C6—H6A \cdots Br1 ^{iv}	0.99	3.02	3.944 (4)	157
C7—H7A \cdots Br1 ^{iv}	0.99	3.02	3.978 (4)	163
C15—H15A \cdots Br2 ⁱⁱⁱ	0.99	2.86	3.503 (4)	123
C15—H15B \cdots Br2 ⁱ	0.99	3.09	3.973 (4)	149

Symmetry codes: (i) $-x+1, -y+1, -z+1$; (ii) $x, -y+3/2, z+1/2$; (iii) $x, -y+3/2, z-1/2$; (iv) $-x, -y+1, -z+1$.